A flexible interpenetrating coordination framework with a bimodal porous functionality

TAPAS KUMAR MAJI*, RYOTARO MATSUDA† AND SUSUMU KITAGAWA‡

Department of Synthetic Chemistry and Biological Chemistry, Graduate School of Engineering, Kyoto University, Katsura, Nishikyo-ku, Kyoto 615-8510, Japan
*Present address: Chemistry and Physics of Materials Unit, Jawaharlal Nehru Center for Advanced Scientific Research, Jakkur, Bangalore-560 064, India
†Present address: Institute for Materials Chemistry and Engineering, Kyushu University, 6-1 Kasuga-koen, Kasuga, Fukuoka, 816-8586, Japan
‡e-mail: kitagawa@sbchem.kyoto-u.ac.jp

Published online: 28 January 2007; doi:10.1038/nmat1827

Introducing a functional part into open-framework materials that tunes the pore size/shape and overall porous activity will open new routes in framework engineering and in the fabrication of new materials. We have designed and synthesized a bimodal microporous twofold interpenetrating network $\{[Ni(bpe)_2(N(CN)_2)](N(CN)_2)(5H_2O)\}_n$ (1), with two types of channel for anionic $N(CN)_2^-$ (dicyanamide) and neutral water molecules, respectively. The dehydrated framework provides a dual function of specific anion exchange of free $N(CN)_2^-$ for the smaller N_3^- anions and selective gas sorption. The N_3-exchanged framework leads to a dislocation of the mutual positions of the two interpenetrating frameworks, resulting in an increase in the effective pore size in one of the counterparts of the channels and a higher accommodation of adsorbate than in the as-synthesized framework (1), showing the first case of controlled sorption properties in flexible porous frameworks.

The design and synthesis of microporous coordination networks with a novel structural topology using the molecular self-assembly approach and constructed using multidentate ligands and a metal centre have been the focus of intense activity[1–5]. Ordered porous frameworks with a large surface area, permanent porosity and high thermal stability have been the central feature during this decade, because of their potential application in the storage of gases[6–9], as catalysts[10–13], in separation[13,14], and in exchange[15] reactions. In addition to such targeted approaches, an approach to create other properties, that is, the characteristics of porous coordination polymers, has been explored, and the most interesting is the dynamic micropore approach, which responds to a chemical stimulus[16–23]. This property can arise in a 'soft' framework showing bistability, whose two states oscillate, and where the system can exist in one of two states for the same external parameter values.

However, rational synthesis of such networks is often thwarted by interpenetration and architectural frailty, which arise from the presence of large linkers, which extend into the distances between the nodes. Therefore, the regulation of this interpenetration to remove any obstacles to porous functionalities is an important challenge in crystal engineering. Recently, an intriguing report claimed that even an interpenetrating framework tends to have a certain porous functionality[16–18,24–26]. Stiff interpenetrating frameworks maintain their structural integrity on guest molecule storage, whereas structural flexibility, such as a mutual framework slide, enables a new type of porous functionality to occur, the so-called controllable gate-opening property[17,18]. Furthermore, ordered porous frameworks, which show specific guest-molecule accommodation or sorption[27–32] or selective exchange[33,34], extend to materials used in practical applications, such as separation, sensing and actuators. The

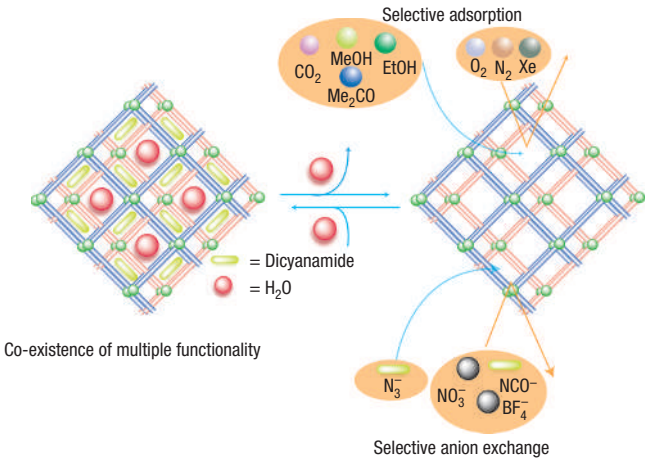

Scheme 1 Robust α-polonium-type three-dimensional interpenetrating porous framework with multiple functionality.

reported data on sorption selectivity are corroborated by the larger kinetic diameter of the adsorbate compared with the dimensions of channel aperture. The particularly versatile applicability of these materials is connected to the interrelated and interdependent coexistence of multiple properties within the same framework[35,36], such as the dual function of specific anion exchange and selective sorption and their control in the same framework, which is unprecedented.

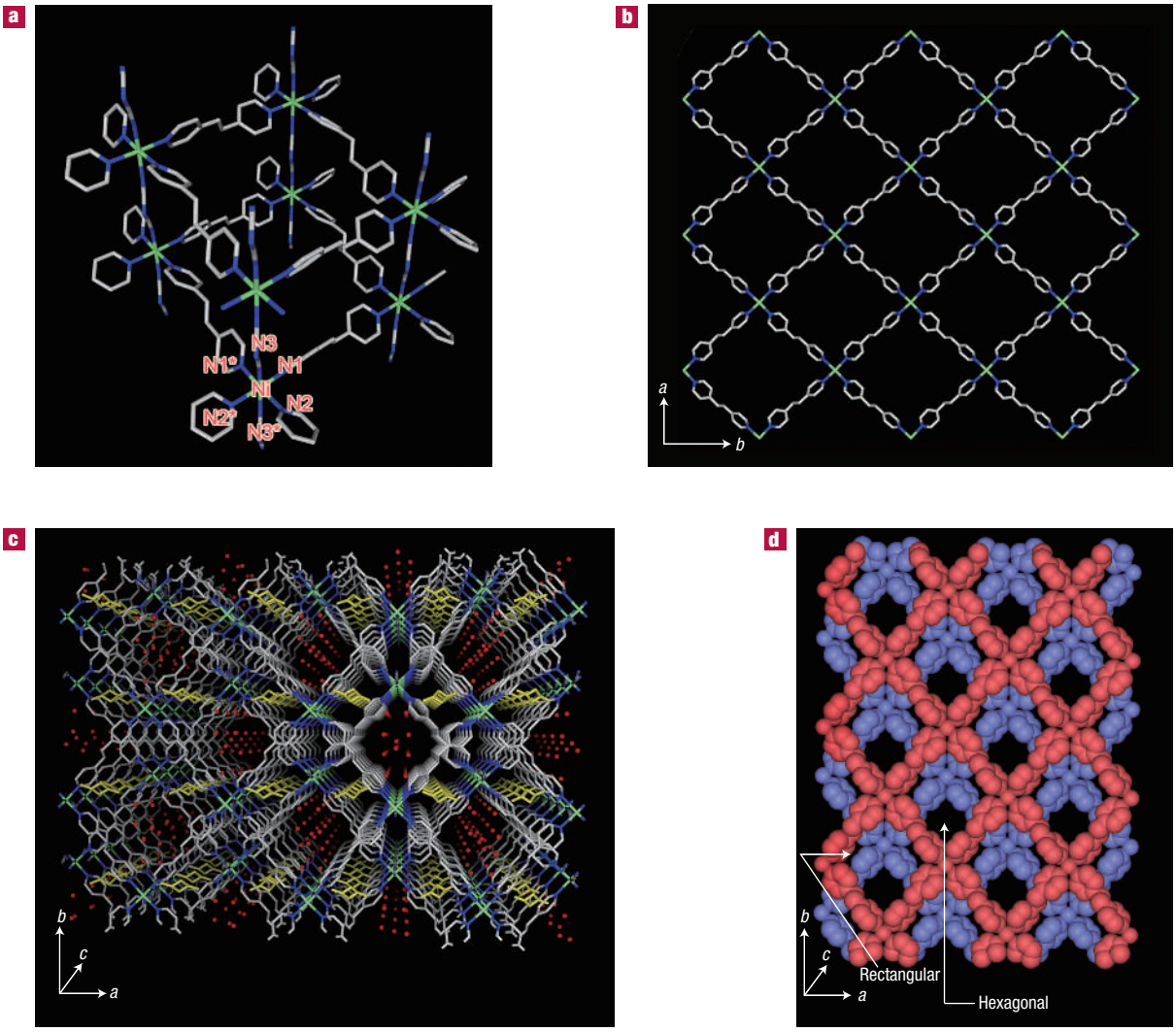

Figure 1 X-ray crystal structure of $\{[Ni(bpe)_2(N(CN)_2)](N(CN)_2)(5H_2O)\}_n$ (1). a, View of the building unit of **1** with atom numbering scheme. **b**, Two-dimensional square grid of $[Ni(bpe)_2]_n$ lying in the crystallographic *ab* plane. **c**, Three-dimensional network of **1** showing two kinds of channel along the crystallographic *c* axis. The rectangular channel accommodates free $N(CN)_2^-$ anions (yellow) and the hexagonal channel is occupied by water molecules (red). **d**, Views of the pore: space-filling diagram of **1** showing twofold interpenetration of a three-dimensional α-polonium-type network with a one-dimensional hexagonal and rectangular channel along the crystallographic *c* axis. The non-coordinated $N(CN)_2^-$ anions and guest water molecules have been omitted for clarity.

Here, we present a robust metal–organic framework with a twofold interpenetrating α-polonium-type network topology, $\{[Ni(bpe)_2(N(CN)_2)](N(CN)_2)(5H_2O)\}_n$ (**1**) (bpe = 1,2-bis(4-pyridyl)ethane; $N(CN)_2^-$ = dicyanamide), which shows a permanent porosity, a high thermal stability and a highly selective sorption, as well as highly selective anion exchange properties (see Scheme 1). The sorption selectivity arises from the interaction between the adsorbates and the pore surface of the adsorbent, whereas exchange selectivity depends on the size, shape and symmetry of the anions. Interestingly, the exchange of the smaller N_3^- anions with $N(CN)_2^-$ anions affects the slippage of the two three-dimensional nets, and results in a considerable increase in the channel dimensions, which is corroborated by the sorption properties. This represents a bimodal functional material in that an anion guest molecule in one channel controls the guest sorption in another channel, the novel porous properties being realized by the flexible interpenetrating framework.

Violet crystals of **1** were obtained on reacting $Ni(NO_3)_2 \cdot 6H_2O$, bpe and $N(CN)_2^-$ in a mixture of water and ethanol. The crystal structure was determined using X-ray crystallography, and the building unit with the atom-labelling scheme is shown in Fig. 1a. In **1**, each octahedral Ni(II) centre sits in a special position attached to four nitrogen atoms (N1, N1*, N2 and N2*) via the four bpe ligands, and two nitrogen atoms (N3 and N3*) via the two $N(CN)_2^-$ anions with a NiN_6 chromophore. The four bpe ligands ligated to each Ni(II) centre form a $[Ni(bpe)_2]_n^{2-}$ two-dimensional sheet in the *ab* plane (Fig. 1b), which is pillared by $N(CN)_2^-$ groups forming a three-dimensional framework (Fig. 1c). A cuboidal box containing eight Ni(II) ions at the corners, connected by four short $N(CN)_2^-$ and eight long bpe linkers, forms the smallest unit of the three-dimensional framework (Fig. 1a). All the bpe ligands are in the *trans* conformation. The Ni–N bond distances are in the range 2.074(5)–2.137(5) Å. The degree of distortion from the ideal octahedral geometry is reflected

in the *cisoid* angles, 85.74(13)–93.70(15)°, and the *transoid* angles 172.70(17)–175.86(14)°. The Ni…Ni separation along the $N(CN)_2^-$ and bpe ligands is 8.63 and 13.53 Å, respectively.

It is worth noting that two independent three-dimensional networks are mutually twofold interpenetrating, forming α-polonium-type network topology (Fig. 1c)[37,38]. The most interesting aspect of the structure is that on interpenetration the framework provides two types of channel: one is a rectangular channel, which accommodates free $N(CN)_2^-$ anions, and the other is a hexagonal channel, which is occupied by water molecules oriented along the crystallographic *c* axis (Fig. 1c,d). The hexagonal channel dimensions are 6.50×4.74 Å^2 and the rectangular channel dimensions are 2.81×0.61 Å^2 (the channel size is measured by considering van der Waals radii for constituting atoms), both of which provide a void space composed of 19.2% of the total crystal volume (Fig. 1d). The C–H…π and π–π interactions, the templating $N(CN)_2^-$ anions and the twofold interpenetration are responsible for stabilizing the overall three-dimensional architecture and topology of the framework.

Thermogravimetric analysis in a nitrogen atmosphere of 1 atm pressure and X-ray powder diffraction (XRPD) measurements were carried out to examine the thermal stability of this porous framework. The stepwise thermogravimetric curve (see Supplementary Information, Fig S1) of **1** indicates that the release of the guest water molecules occurred at ~75 °C to give the dehydrated form, $\{[Ni(bpe)_2(N(CN)_2)](N(CN)_2)\}_n$ (**1a**), which is stable up to ~150 °C. Therefore, the dehydration can be accomplished by heating at the temperature range between 75 and 150 °C. On further heating, one bpe molecule is lost at a temperature of ~190 °C, forming a sky-blue compound. On further heating, another bpe molecule is released (~350 °C), and then the compound decomposes to form unidentified products. No chemical decomposition was observed between the dehydration and ligand release temperatures. Figure 2 shows XRPD patterns simulated from the X-ray single-crystal data of as-synthesized **1**, dehydrated **1a** and rehydrated **2**. The XRPD pattern of **1a** is similar to that of **1**, indicating that the framework is robust, and is maintained even without any guest water molecules being present.

It is interesting to note that **1** retains its single crystallinity, even after the removal of the guest water molecules by heating the crystal at 100 °C under an Ar atmosphere for a period of 2 h. This is accompanied by a sharp change in colour from violet to deep blue (Fig. 3). The X-ray structure of the dehydrated crystal (**1a**) indicates that there is no significant change in the unit-cell parameters, and the porous structure with a three-dimensional interpenetrating framework is retained. It is worth mentioning that on dehydration the two closely packed interpenetrating networks undergo stress relaxation, which is attributed to the expansion of the channel size (hexagonal channel = 6.78×4.78 Å^2 and rectangular channel = 2.87×0.69 Å^2) to provide a void space composing 21.7% of the total crystal volume (see Supplementary Information, Fig S2). The distinct colour change is attributable to a slight change in the Ni–N bond length, and also to a change in the N–Ni–N bond angle (see Supplementary Information, Tables S1,S2). When a dehydrated single crystal of **1a** was exposed to the ambient atmosphere for a period of more than 1 day, the blue colour of the crystal returned to the original violet colour (Fig. 3). The same phenomenon was also observed in the case of a powdered sample when it was exposed to water vapour. The crystal structure of the rehydrated state (**2**) showed the same structure as **1** (see Supplementary Information, Fig S2).

Sorption experiments with different adsorbates were carried out to confirm the permanent porosity of framework **1**. It was observed that a significant amount of carbon dioxide sorption

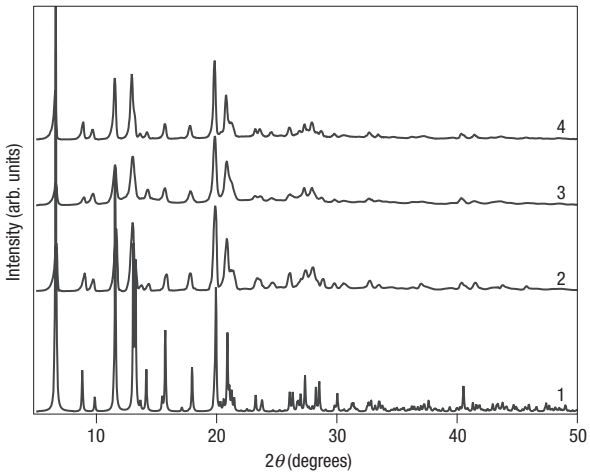

Figure 2 XRPD patterns in different states. Curve 1, Simulated (**1**). Curve 2, As synthesized (**1**). Curve 3, Drying *in vacuo* at 85 °C for 4 h (**1a**). Curve 4, **1a** exposed to water vapour for 24 h (**2**).

(surface area = 17.9 Å^2, kinetic diameter = 3.3 Å, molecular area is calculated from the liquid density, assuming spherical symmetry and hexagonal close packing)[39,40] occurred at 195 K (Fig. 4a). The most interesting phenomenon was observed with methanol (18.0 Å^2), which showed a stepwise sorption with a large hysteresis (Fig. 4b). The profile shows that after an initial adsorption of about one molecule of methanol at point 1 (relative methanol vapour pressure, $P/P_0 = 0.44$) per unit pore, another abrupt molecule adsorption occurred at point 2 ($P/P_0 = 0.9$). The desorption curve did not trace the adsorption curve any longer, and suddenly dropped from point 3 ($P/P_0 = 0.15$) onwards. This kind of hysteretic sorption results in an observation of a dynamic structural transformation from dehydrated to guest-occupied structure. The XRPD patterns of dehydrated **1** at different relative methanol vapour pressures of 0.2, 0.5 and 1.0 did not show distinctive differences among them (see Supplementary Information, Fig. S3). The small changes in the crystal accompanying successive guest accommodations are characteristic of the stiffness of the three-dimensional grid motif, whereas the other cases have a combination of the stiff and flexible motifs, giving rise to a remarkable breathing phenomenon[41]. The first step is associated with the presence of the predominant adsorption site in the framework. The as-synthesized structure reveals that three types of guest water molecule exist, and one of them (O3) strongly interacts with the pillar $N(CN)_2^-$ anion of the pore wall (O3…N5, 2.25 Å) with hydrogen bonding in comparison with the O1 and O2. Analogously, methanol is first adsorbed in this site and the following molecule of methanol is adsorbed in the rest of the binding sites, resulting in a stepwise and hysteretic adsorption profile. This type of adsorption behaviour has been reported for the carbon dioxide sorption profile in MIL-53 with two different adsorption sites[23]. The micropore filling of vapours is described by the Dubinin–Radushkevich equation, which was used to analyse the resulting isotherm, and to characterize the porous properties. The micropore volume from carbon dioxide adsorption from the Dubinin–Radushkevich data was about 185.7 m^2 g^{-1}, which is accessible for 0.8 molecules of carbon dioxide per formula unit. Similarly, at 298 K, water (10.5 Å^2), ethanol (23.1 Å^2) and acetone (26.8 Å^2) can diffuse into the micropores of **1a** (Fig. 5), and all the profiles show hysteretic sorption behaviour (see Supplementary

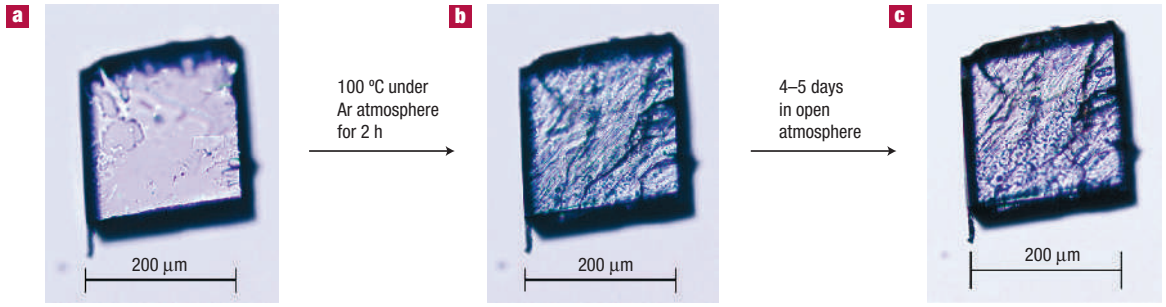

Figure 3 Morphology of the crystal of $\{[Ni(bpe)_2(N(CN)_2)](N(CN)_2)(5H_2O)\}_n$ in different states. a, As-synthesized crystal (violet, **1**). **b**, Dehydrated crystal (deep blue, **1a**). **c**, Rehydrated crystal (violet, **2**).

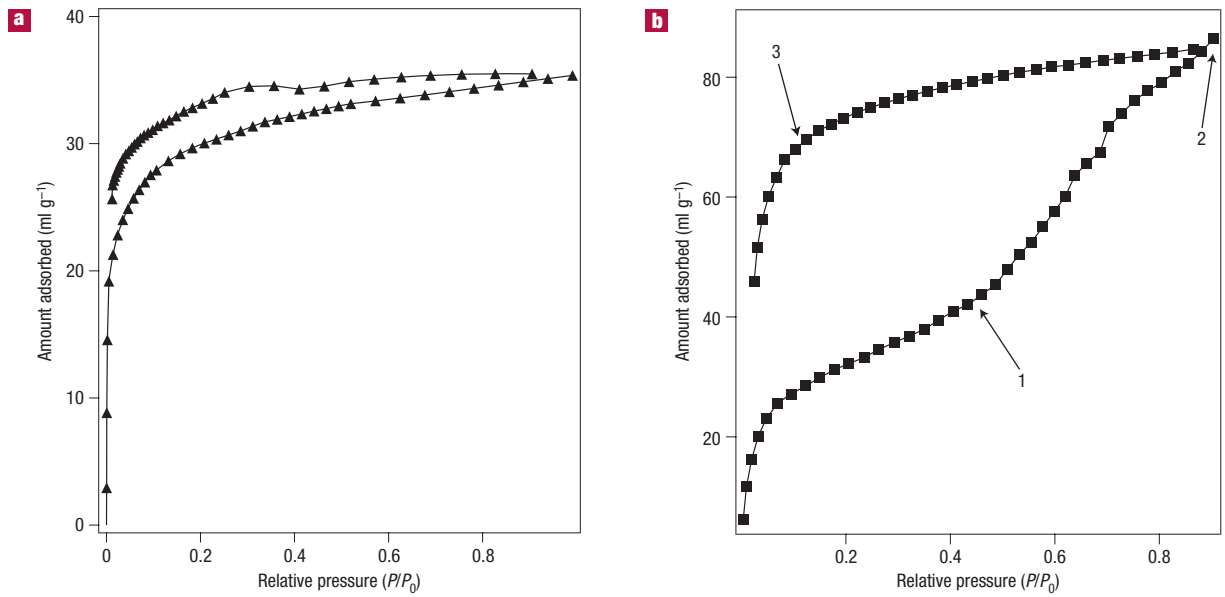

Figure 4 Adsorption isotherm for vapour adsorption in $\{[Ni(bpe)_2(N(CN)_2)](N(CN)_2)\}_n$ (1a). a, Carbon dioxide (195 K). **b**, Methanol (298 K). P/P_0 is the relative pressure, where P_0 is the saturated vapour pressure of the adsorbate at the respective temperature. Points 1–3 are discussed in the text.

Information, Fig. S4) correlating with the diversity of the binding sites. The amount of adsorption was calculated using the Dubinin–Radushkevich equation, which shows that for every Ni(II) atom 2.5 water molecules, 2 methanol molecules, 0.72 ethanol molecules and 0.75 acetone molecules can be adsorbed into a micropore. On the other hand, the adsorption of water began in the higher-P/P_0 region, gradually increased and ended without saturation being reached, correlating with the lower value of water adsorption compared with the number of water molecules accommodated in the as-synthesized framework **1**. This result indicates that the adsorbate–adsorbate interaction is higher relative to the apohost–adsorbate interaction in the case of water, compared with methanol.

Despite the stable framework and an adequate effective pore size, to our surprise no nitrogen (16.3 Å^2, 3.64 Å) or oxygen (14.1 Å^2, 3.46 Å) diffusion into the micropores was observed at 77 K (Fig. 5, curves 4 and 5). Interestingly, a significant carbon dioxide uptake was observed at 195 K, despite its similar size to oxygen (Fig. 4a). It is noteworthy that we also measured the adsorption of xenon (surface area = 17.1 Å^2, 3.96 Å) at 195 K to study the effect of temperature. However, only surface adsorption occurred (Fig. 5, curve 6). This type of selectivity is unprecedented and unique, as the channel aperture of **1a** is large enough to accommodate nitrogen, oxygen and xenon, and the reported sorption selectivity in the literature correlates with this size effect[28–32]. It is probable that the oxygen and nitrogen adsorbates at 77 K interact very strongly with the pore windows, which block other molecules from passing into the pore, as the framework has no other additional open channel along the *a* and *b* axes. In the case of carbon dioxide sorption (at 195 K), such interactions are overcome by the thermal energy and the framework host, which contains Ni(II), polar groups and π-electron clouds from the bpe ligands inside the pores. This gives rise to an electric field, which is effective in carbon dioxide sorption. Such dipole–induced-dipole interactions, where the quadrupole moment of carbon dioxide interacts with the electric field gradient, make a further contribution to the potential energy of adsorption for carbon dioxide[31].

As described above, the as-synthesized framework **1** contains one free $N(CN)_2^-$ anion per Ni(II) unit in the rectangular channel, and because **1** is not soluble in common solvents this framework

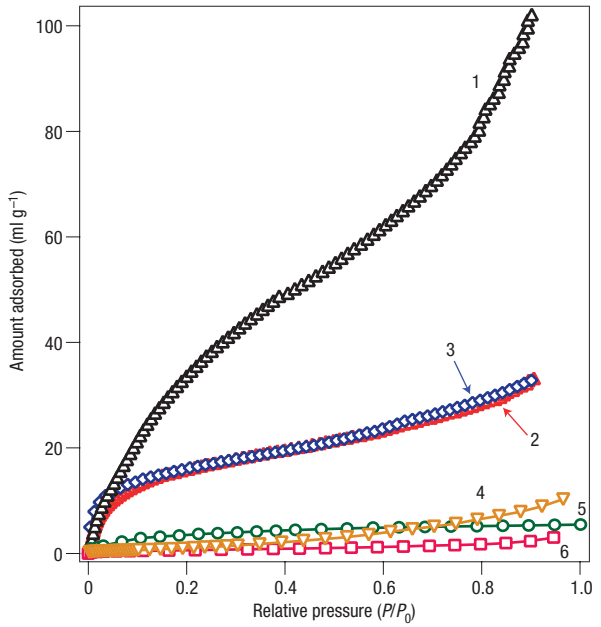

Figure 5 Adsorption isotherm for vapour adsorption in $\{[Ni(bpe)_2(N(CN)_2)](N(CN)_2)\}_n$ (1a). Curve 1, Water (298 K). Curve 2, Ethanol (298 K). Curve 3, Acetone (298 K). Curve 4, Nitrogen (77 K). Curve 5, Oxygen (77 K). Curve 6, Xenon (195 K). P/P_0 is the relative pressure, where P_0 is the saturated vapour pressure of the adsorbate at the respective temperature.

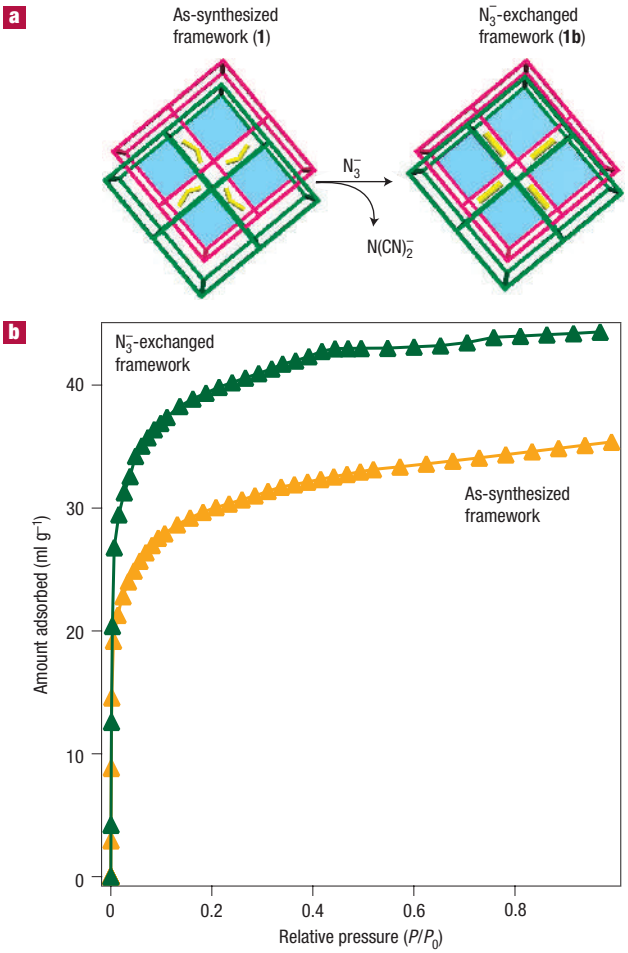

Figure 6 Nanospace engineering by anion exchange. a, Schematic diagram of the pore size controlled by the anion exchange. **b**, Comparison of carbon dioxide adsorption isotherm in as-synthesized (yellow) $\{[Ni(bpe)_2(N(CN)_2)](N(CN)_2)\}_n$ (**1a**) and N_3-exchanged (green) $\{[Ni(bpe)_2(N(CN)_2)](N_3)\}_n$ frameworks.

was expected to undergo anion exchange. As the dimensions of the channel are small, and $N(CN)_2^-$ is almost a linear ligand, we chose smaller anions, such as N_3^-, NCO^-, NO_3^- and BF_4^-, compared with the larger anions, such as ClO_4^- and PF_6^-, for the exchange experiment. The insoluble violet crystals of **1** were immersed in excesses of aqueous NaN_3, NaNCO, $NaBF_4$ and $NaNO_3$ solutions separately, and after a period of 1 day we observed the violet crystals change to a light green colour (see Supplementary Information, Fig. S5) in the case of NaN_3 solution, whereas no colour change occurred in the cases of NaNCO, $NaNO_3$ and $NaBF_4$ solutions. Each product was separated and characterized using elemental analysis, infrared spectroscopy and XRPD measurements. The green crystals from the N_3 solution showed that an additional intense broad band occurred at 2,061 cm^{-1}, corresponding to the asymmetric stretching frequency of the N_3^- anion, $\nu_{as}(N_3)$, compared with the as-synthesized compound (see Supplementary Information, Fig. S6). The XRPD patterns were similar to the as-synthesized compound, except the splitting of the (111) peak, which is in the plane that contains the free $N(CN)_2^-$ anions in the as-synthesized compound, suggesting an exchange with N_3^- anions had occurred (see Supplementary Information, Fig. S7). The elemental analysis data confirm the formulation of $\{[Ni(bpe)_2(N(CN)_2)](N_3)(5H_2O)\}_n$, corroborating the quantitative exchange of the free $N(CN)_2^-$ anions with the N_3^- anions. However, X-ray diffraction images of anion-exchanged crystals did not show clear spots owing to the loss of their single crystallinity (see Supplementary Information, Fig. S8). It is noteworthy that the N_3-exchange process is irreversible. The compound formed in the NCO^-, NO_3^- and BF_4^- solutions did not show any change in colour, and the elemental analysis, infrared spectroscopy and XRPD data (see Supplementary Information, Figs S6,S7) suggest that NCO^-, NO_3^- and BF_4^- cannot exchange with $N(CN)_2^-$ anions. This may be due to the symmetries, shapes and sizes of the NCO^-, NO_3^- and BF_4^- ions, which are different from those of the $N(CN)_2^-$ anion, and shows that the framework can undergo only size-, shape- and symmetry-selective anion exchange (Fig. 6a)[33,34]. It is interesting to note that carbon dioxide sorption was carried out by the N_3-exchanged framework, which shows that about 10 ml g^{-1} more carbon dioxide (from the Dubinin–Radushkevich equation) is adsorbed compared with the as-synthesized $N(CN)_2^-$ anion compound, corroborating the increase in the effective pore size or the framework's permanent porosity (Fig. 6b). The micropore-volume carbon dioxide adsorption from the Dubinin–Radushkevich graph was about 243.15 m^2 g^{-1}, which means that the micropore is accessible for one carbon dioxide molecule per formula unit. This is possible because the N_3^- anion is smaller than the $N(CN)_2^-$ anion, which causes a bias in the mutual position of the two three-dimensional nets due to sliding, and this results in an increase in channel size, or more space to accommodate a larger number of carbon dioxide molecules compared with **1a**. This anion exchange can control the framework structure, as well as the porosity; it is corroborated by sorption studies and shows the

'nanospace engineering by anion exchange' phenomenon, which is unique (Fig. 6).

In conclusion, we have synthesized a novel α-polonium-type metal–organic hybrid framework containing Ni(II), which has a permanent porosity and a high thermal stability. It is constructed from two interpenetrating three-dimensional networks. The retention of single crystallinity on dehydration and rehydration[42–44] is accompanied by a change in colour (thermochromism), which is unique in porous coordination polymers. These materials have potential applications in thermal sensing. The robust dehydrated framework shows a highly selective sorption behaviour towards different adsorbates that is not dependent on the pore size, which shows that the adsorbate–adsorbent interaction is very important in the selective sorption phenomenon. The as-synthesized compound selectively exchanges the free $N(CN)_2^-$ anions with N_3^- anions, concomitant with an increase in permanent porosity and a colour change from violet to green. In the case of NCO^-, NO_3^- and BF_4^- anions, the framework does not respond to any change. This anion exchange controls the overall framework functionality, and thus new porous materials made of two simple building blocks may find useful applications in gas separation, sensor and anion exchange applications, that is, bifunctionality in one compound, paving the way for the fabrication of new materials.

METHODS

SYNTHESIS OF $\{[Ni(bpe)_2(N(CN)_2)](N(CN)_2)(5H_2O)\}_n$ (1)

An aqueous solution (25 ml) of $Na(N(CN)_2)$ (1 mmol, 0.089 g) was mixed with an ethanolic solution (25 ml) of bpe (1 mmol, 0.184 g) and stirred for 20 min to mix well. $Ni(NO_3)_2 \cdot 6H_2O$ (0.5 mmol, 0.145 g) was dissolved in 50 ml water and 2 ml of this Ni(II) solution was slowly and carefully layered on the above mixed ligand solution. The dark-violet block-shaped crystals were obtained after one week. The crystals were separated and washed with ethanol–water (1:1) mixture and dried. The bulk amount of the material was obtained on mixing the ethanolic solution of bpe into the aqueous solution of $Ni(NO_3)_2 \cdot 6H_2O$ and $NaN(CN)_2$. Yield 80%. (Elemental analysis calculated for $C_{28}H_{34}N_{10}NiO_5$ (**1**) C, 51.79; H, 5.24; N, 21.58; found C, 52.24; H, 4.72; N, 21.37.)

STRUCTURAL STUDIES

X-ray structure determination for **1**,**1a** and **2** was carried out as follows. Measurements were recorded on a Rigaku mercury CCD (charge-coupled device) diffractometer with graphite-monochromated Mo Kα radiation ($\lambda = 0.71069$ Å) and a CCD two-dimensional detector. All the structures were solved by direct methods by using the SIR97 program and expanded by using Fourier techniques. For all three complexes (**1**, **1a** and **2**), hydrogen atoms were placed in the ideal positions and refined isotropically.

The oxygen atoms O1, O2 and O3 of water molecules in the cases of **1** and **2** and C3 and C4 atoms of **1a** were refined isotropically. The nitrogen and carbon atoms of the non-coordinated dicyanamide ligand were also refined isotropically in all three cases. CCDC-615994 (**1**), CCDC-615995 (**1a**) and CCDC-615996 (**2**) contain the supplementary crystallographic data for this paper. These data can be obtained free of charge via www.ccdc.cam.ac.uk/conts/retrieving.html (or from the Cambridge Crystallographic Data Centre, 12 Union Road, Cambridge CB21EZ, UK; fax (+44)1223-336-033; or deposit@ccdc.cam.ac.uk).

GAS ADSORPTION MEASUREMENT

The sorption isotherm measurements for nitrogen, oxygen (at 77 K), xenon and carbon dioxide (at 195 K) gases and water, methanol, ethanol and acetone solvents (at 298 K) were carried out by using an automatic volumetric adsorption apparatus (Belsorp 18; BEL). A known weight (150–200 mg) of the as-synthesized sample was placed in the quartz tube, then, before measurements, the sample was dried under high vacuum at 358 K for 5 h to remove the solvated water molecules. The adsorbate was placed into the sample tube, then the change of the pressure was monitored and the degree of adsorption was determined by the decrease of the pressure at the equilibrium state.

Received 14 September 2006; accepted 4 December 2006; published 28 January 2007.

References

1. Kitagawa, S., Kitaura, R. & Noro, S. I. Functional porous coordination polymers. *Angew. Chem. Int. Edn* **43**, 2334–2375 (2004).
2. Yaghi, O. M. *et al.* Reticular synthesis and the design of new materials. *Nature* **423**, 705–714 (2003).
3. Bradshaw, D., Claridge, J. B., Cussen, E. J., Prior, T. J. & Rosseinsky, M. J. Design, chirality, and flexibility in nanoporous molecule-based materials. *Acc. Chem. Res.* **38**, 273–282 (2005).
4. Férey, G., Mellot-Draznieks, C., Serre, C. & Millange, F. Crystallized frameworks with giant pores: Are there limits to the possible? *Acc. Chem. Res.* **38**, 217–225 (2005).
5. Janiak, C. Engineering coordination polymers towards applications. *Dalton Trans.* 2781–2804 (2003).
6. Férey, G. *et al.* A chromium terephthalate-based solid with unusually large pore volumes and surface area. *Science* **309**, 2040–2042 (2005).
7. Rowsell, J. L. C. & Yaghi, O. M. Strategies for hydrogen storage in metal–organic frameworks. *Angew. Chem. Int. Edn* **44**, 4670–4679 (2005).
8. Noro, S. I., Kitagwa, S., Kondo, M. & Seki, K. A new, methane adsorbent, porous coordination polymer $[\{Cu(SiF_6)(4,4'\text{-bipyridine})_2\}_n]$. *Angew. Chem. Int. Edn* **39**, 2082–2084 (2000).
9. Kondo, M., Yoshitomi, T., Seki, K., Matsuzaka, H. & Kitagawa, S. Three-dimensional framework with channeling cavities for small molecules: $\{[M_2(4,4'\text{-bpy})_3(NO_3)_4].xH_2O\}_n$ (M = Co, Ni, Zn). *Angew. Chem. Int. Edn* **36**, 1725–1726 (1997).
10. Ohmori, O. & Fujita, M. Heterogeneous catalysis of a coordination network: cyanosilylation of imines catalyzed by a Cd(II)-(4,4′-bipyridine) square grid complex. *Chem. Commun.* 1586–1587 (2004).
11. Wu, C.-D., Hu, A., Zhang, L. & Lin, W. A homochiral porous metal–organic framework for highly enantioselective heterogeneous asymmetric catalysis. *J. Am. Chem. Soc.* **127**, 8940–8941 (2005).
12. Chang, J.-S. *et al.* Nanoporous metal containing nickel phosphates: A class of shape selective catalyst. *Angew. Chem. Int. Edn* **43**, 2819–2822 (2004).
13. Seo, J. S. K. *et al.* A homochiral metal–organic porous material for enantioselective separation and catalysis. *Nature* **404**, 982–986 (2000).
14. Pan, L., Olson, D. H., Ciemnolonski, L. R., Heddy, R. & Li, J. Separation of hydrocarbons with a microporous metal–organic framework. *Angew. Chem. Int. Edn* **45**, 616–619 (2006).
15. Min, K. S. & Suh, M. P. Silver(I)-polynitrile network solids for anion exchange: Anion-induced transformation of supramolecular structure in the crystalline state. *J. Am. Chem. Soc.* **122**, 6834–6840 (2000).
16. Halder, G. H., Kepert, C. J., Moubaraki, B., Murray, K. S. & Cashion, J. D. Guest dependent spin crossover in a nanoporous molecular framework material. *Science* **298**, 1762–1765 (2002).
17. Kitaura, R., Seki, K., Akiyama, G. & Kitagawa, S. Porous coordination-polymer crystals with gated channels specific for supercritical gases. *Angew. Chem. Int. Edn* **42**, 428–431 (2003).
18. Seki, K. Dynamic channels of a porous coordination polymer responding to external stimuli. *Phys. Chem. Chem. Phys.* **4**, 968–1971 (2002).
19. Lee, E. Y., Jang, S. Y. & Suh, M. P. Multifunctionality and crystal dynamics of a highly stable, porous metal–organic framework $[Zn_4O(NTB)_2]$. *J. Am. Chem. Soc.* **127**, 6374–6381 (2005).
20. Biradha, K. & Fujita, M. A spring like 3D-coordination network that shrinks or swells in a crystal-to-crystal manner upon guest removal or readsorption. *Angew. Chem. Int. Edn* **41**, 3392–3395 (2002).
21. Matsuda, R. *et al.* Guest shape-responsive fitting of porous coordination polymer with shrinkable framework. *J. Am. Chem. Soc.* **126**, 14063–14070 (2004).
22. Cussen, E. J., Claridge, J. B., Rosseinsky, M. J. & Kepert, C. J. Flexible sorption and transformation behavior in a microporous metal–organic framework. *J. Am. Chem. Soc.* **124**, 9574–9581 (2002).
23. Bourrelly, S. *et al.* Different adsorption behaviors of methane and carbon dioxide in the isotypic nanoporous metal terephthalates MIL-53 and MIL-47. *J. Am. Chem. Soc.* **127**, 13519–13521 (2005).
24. Reineke, T. M., Eddaoudi, M., Moler, D., O'Keeffe, M. & Yaghi, O. M. Large free volume in maximally interpenetrating networks: The role of secondary building units exemplified by $Tb_2(ADB)_3[(CH_3)_2SO]_4.16[(CH_3)_2SO]$. *J. Am. Chem. Soc.* **122**, 4843–4844 (2000).
25. Chen, B., Eddaoudi, M., Hyde, S. T., O'Keeffe, M. & Yaghi, O. M. Interwoven metal–organic framework on a periodic minimal surface with extra large pores. *Science* **291**, 1021–1023 (2001).
26. Kesanli, B. *et al.* Highly interpenetrated metal–organic frameworks for hydrogen storage. *Angew. Chem. Int. Edn* **44**, 72–75 (2005).
27. Matsuda, R. *et al.* Highly controlled acetylene accommodation in a metal–organic microporous material. *Nature* **436**, 238–241 (2005).
28. Kuznicki, S. M. *et al.* A titanosilicate molecular sieve with adjustable pores for size-selective adsorption of molecules. *Nature* **412**, 720–723 (2001).
29. Dinca, M. & Long, J. R. Strong H_2 binding and selective gas adsorption within the microporous coordination solid $Mg_3(O_2C\text{-}C_{10}H_6\text{-}CO_2)_3$. *J. Am. Chem. Soc.* **127**, 9376–9377 (2005).
30. Dybtsev, D. N., Chun, H., Yoon, S. H., Kim, D. & Kim, K. Microporous manganese formate: A simple metal–organic porous material with high framework stability and high selective gas sorption properties. *J. Am. Chem. Soc.* **126**, 32–33 (2004).
31. Pan, L. *et al.* Porous lanthanide-organic frameworks: Synthesis, characterization, and unprecedented gas adsorption properties. *J. Am. Chem. Soc.* **125**, 3062–3067 (2003).
32. Maji, T. K., Uemura, K., Chang, H.-C., Matsuda, R. & Kitagawa, S. Expanding and shrinking porous modulation based on pillared-layer coordination polymers showing selective guest adsorption. *Angew. Chem. Int. Edn* **43**, 3269–3272 (2004).
33. Muthu, S., Yip, J. H. K. & Vittal, J. J. Coordination network of Ag(I) and N, N′-bis(3-pyridine-carboxamide)-1,6-hexane: Structure and anion exchange. *J. Chem. Soc. Dalton Trans.* 4561–4568 (2002).
34. Lee, E., Kim, J., Heo, J., Whang, D. & Kim, K. A two dimensional polyrotaxane with large cavities and channels: A novel approach to metal–organic open-frameworks by using supramolecular building blocks. *Angew. Chem. Int. Edn* **40**, 399–402 (2001).
35. Kurmoo, M., Kumagai, H., Hughes, S. M. & Kepert, C. J. Reversible guest exchange and ferrimagnetism ($T_c = 60.5$ K) in a porous cobalt(II)-hydroxide layer structure pillared with *trans*-1,4-cyclohexanedicarboxylate. *Inorg. Chem.* **42**, 6709–6722 (2003).
36. Guillou, N., Livage, C., Drillon, M. & Férey, G. The chirality, porosity, and ferromagnetism of a 3D nickel glutarate with intersecting 20-membered ring channels. *Angew. Chem. Int. Edn* **42**, 5314–5317 (2003).
37. Abrahams, B. F., Batten, S. R., Hamit, H., Hoskins, B. F. & Robson, R. A cubic (3,4)-connected net with large cavities in solvated $[Cu_3(tpt)_4](ClO_4)_3$ (tpt = 2,4,6-Tri(4-pyridyl)-1,3,5-triazine). *Angew. Chem. Int. Edn Engl.* **35**, 1690–1692 (1996).
38. Tong, M. L. *et al.* A novel three-dimensional coordination polymer constructed with mixedvalence dimeric copper(I,II) units. *Chem. Commun.* 428–429 (2003).
39. Webster, C. E., Drago, R. S. & Zerner, M. C. Molecular dimensions for adsorptives. *J. Am. Chem. Soc.* **120**, 5509–5516 (1998).
40. Beck, D. W. *Zeolite Molecular Sieves* (Wiley, New York, 1974).

41. Llewellyn, P. L., Bourrelly, S., Serre, C, Filinchuk, Y. & Férey, G. How hydration drastically improves adsorption selectivity for CO_2 over CH_4 in the flexible chromium terephthalate MIL-53. *Angew. Chem. Int. Edn* **45**, 7751–7754 (2006).
42. Rather, B. & Zaworotko, M. J. A 3D metal–organic network, [Cu_2(glutarate)$_2$(4, 4′-bipyridine)], that exhibits single-crystal to single-crystal dehydration and rehydration. *Chem. Commun.* 830–831 (2003).
43. Takaoka, K., Kawano, M., Tominaga, M. & Fujita, M. In-situ observation of a reversible single-crystal-to-single-crystal apical-ligand-exchange reaction in hydrogen-bonded 2D coordination network. *Angew. Chem. Int. Edn* **44**, 2151–2154 (2005).
44. Lee, E. Y. & Suh, M. P. A robust porous material constructed of linear coordination polymer chains: Reversible single-crystal-to-single-crystal transformation upon dehydration and rehydration. *Angew. Chem. Int. Edn* **43**, 2798–2801 (2004).

Acknowledgements

This work was supported by Grants-in-Aid for Scientific Research in a Priority Area 'Chemistry of coordination space' (434) and a CREST/JST programme from the Ministry of Education, Culture, Sports, Science and Technology, Government of Japan.
Correspondence and requests for materials should be addressed to S.K.
Supplementary Information accompanies this paper on www.nature.com/naturematerials.

Competing financial interests

The authors declare that they have no competing financial interests.